Misfit Stress in Radial Core-Shell Nanowires with Diffuse Interface Boundaries

A.S. Khramov[1], S.A. Krasnitckii[1–4], A.M. Smirnov[1,*]

[1] Institute of Advanced Data Transfer Systems, ITMO University, Kronverkskiy pr. 49, St. Petersburg 197101, Russia

[2] Laboratory of Nanomaterials Mechanics and Theory of Defects, Institute for Problems in Mechanical Engineering, Russian Academy of Sciences, Bolshoi 61, Vasil. Ostrov, St. Petersburg,199178, Russia

[3] Research Laboratory of Mechanics of New Nanomaterials, Peter the Great St. Petersburg Polytechnic University, Polytekhnicheskaya 29, St. Petersburg, 195251, Russia

[4] Department of Computational Methods in Continuum Mechanics, St. Petersburg State University, Universitetskaya emb. 7-9, St. Petersburg, 199034, Russia

Abstract

The elastic models of radial core-shell nanowires with diffuse interphase boundaries are suggested. The concept of eigenstrain is employed to consider a misfit stress distribution induced by diffusive interfaces with different range of distinctness. The eigenstrain profile described by the misfit parameter is approximated by piecewise-linear, error and arctangent functions. For these approximations the elastic stresses in core-shell nanowires are analytically derived, illustrated with plots and discussed in detail.

1. INTRODUCTION

In recent years core-shell nanowires (NWs) with diffuse interphase boundaries (IPhBs) have attracted an increasing attention of experimenters, technologists [1–4] and theorists [2,4–8]. As the sharp IPhBs with atomically distinct interface are hardly synthesized in practice due to reservoir effect in the catalyst droplet [9], the diffuse IPhBs seems to be more perspective for investigation. For both types of IPhBs the elastic stress and strain caused by the lattice mismatch at the interface between various core and shell materials affect functional properties of the NWs and can lead to the generation of crystal structural defects [10].

The interface indistinctness attributed to the diffuse IPhBs and driven by the mutual diffusion penetration of core and shell atoms, deteriorates the electron and optical properties of these heterostructures [2,5]. Nevertheless, this phenomenon inhibits (prevents) the formation of the misfit defects due to reduction of the strain energy of the lattice mismatch [6,7]. Therefore, the strict theoretical models describing the coherent stress-strain state in NWs with IPhBs are deemed to be essential to investigate the physical foundations of misfit stress relaxation due to the nucleation and evolution of defects in modern electronic and optoelectronic devices.

To date, the theoretical models describing the stress-strain state in axial NWs with a diffuse interface have been developed [6–8], while an elastic model of radial NWs have not been suggested yet. Besides, the available theoretical model of misfit stress relaxation in core-shell heterostructures [11–26] employs the analytical expressions of the elastic stress induced by eigenstrain defined by Heaviside theta function.

This work aims at providing the theoretical model describing the misfit stress of core-shell NWs containing the diffuse IPhBs with different range of distinctness. The piecewise-linear, error and arctangent function approximations of eigenstrain profile are considered to obtain analytically components of elastic stress of radial core-shell NWs.

2. MODEL

We consider a cylindrical core-shell NW of radius b containing the diffuse IPhB of radius a consisting of materials with the same elastic constants (shear modulus μ and

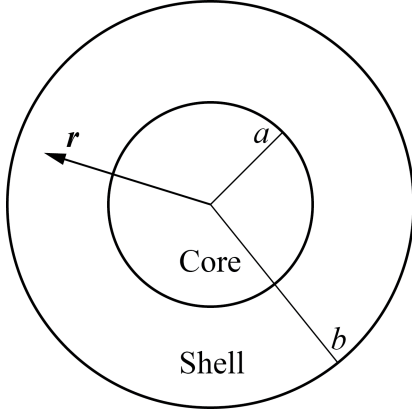* Corresponding author: A.M. Smirnov, e-mail: smirnov.mech@gmail.com

Fig. 1. Sketch of cross section of a radial core-shell NW with outer radius *b* and core radius *a*.

Poisson ratio ν), but with the different core and shell lattice constants a_c and a_s respectively (see Fig. 1). In this NW the lattice mismatch between core and shell materials induces an elastic strain and stress which could be elucidated in terms of eigenstrain deformation $\varepsilon_{ij}^{(pl)}$. Generally, the parameter $\varepsilon_{ij}^{(pl)}$ as a function of the radial coordinate is responsible for the interface distinctness, i.e., diffusion penetration of core atoms into the shell domain, and vice versa.

According to the concept of eigenstrain, the total strain of an elastic cylinder subjected to the residual strain can be decomposed as:

$$e_{ij} = \varepsilon_{ij}^{(el)} + \varepsilon_{ij}^{(pl)}, \tag{1}$$

where $\varepsilon_{ij}^{(el)}$ are the components of elastic stress tensor, $\varepsilon_{ij}^{(pl)} = f\delta_{ij}$ is the dilatational misfit of NW, $f = f(r)$ is a misfit profile determining disturbance of the eigenstrain inside the NW and δ_{ij} is Kronecker delta ($\delta_{ij} = 1$ for $i = j$, $\delta_{ij} = 0$ for $i \neq j$).

Taking into consideration the axial-symmetry of the problem the non-zero components of the total strain tensor in cylindrical coordinate system can be expressed through the displacement with following relations:

$$e_{rr} = \frac{\partial u}{\partial r}, \tag{2a}$$

$$e_{\theta\theta} = \frac{u}{r}, \tag{2b}$$

$$e_{zz} = \frac{\partial u}{\partial z}, \tag{2c}$$

where $u = u_r(r)$ is radial displacement of NW. It is worth noting that axial strain e_{zz} does not depend on either *r* or *z*, i.e., the Eq. (2c) can be rewritten as e_{zz} = const.

The non-zero components of elastic stress tensor σ_{ij} can be obtained by the Hooke law:

$$\sigma_{rr} = 2\mu \left[e_{rr} + \frac{\nu}{1-2\nu} e - \frac{1+\nu}{1-2\nu} f(r) \right], \tag{3a}$$

$$\sigma_{\theta\theta} = 2\mu \left[e_{\theta\theta} + \frac{\nu}{1-2\nu} e - \frac{1+\nu}{1-2\nu} f(r) \right], \tag{3b}$$

$$\sigma_{zz} = 2\mu \left[e_{zz} + \frac{\nu}{1-2\nu} e - \frac{1+\nu}{1-2\nu} f(r) \right], \tag{3c}$$

where $e = e_{rr} + e_{\theta\theta} + e_{zz}$. Besides, the stress tensor components have to satisfy the first equilibrium equation:

$$\frac{\partial \sigma_{rr}}{\partial r} + \frac{\sigma_{rr} - \sigma_{\theta\theta}}{r} = 0. \tag{4}$$

Finally, introduce Eqs. (3) in Eq. (4) with respect to Eqs. (2) and $\partial e_{zz}/\partial r = 0$ one can obtain the differential equation for displacement:

$$\frac{d^2 u}{dr^2} + \frac{1}{r}\frac{du}{dr} - \frac{u}{r^2} = \frac{1+\nu}{1-\nu}\frac{df}{dr}. \tag{5}$$

The solution of Eq. (5) is well-known and can be written in the following form:

$$u = Ar + B\frac{1}{r} + \frac{1+\nu}{1-\nu}\frac{1}{r}\int_0^r f(\rho)\rho d\rho, \tag{6}$$

where *A* and *B* are unknown coefficients. Taking into account the Eqs. (2) and Eq. (6) the components of stress tensor (3) can be rewritten:

$$\sigma_{rr} = \tilde{A} - \tilde{B}\frac{1}{r^2} - 2\mu\frac{1+\nu}{1-\nu}\frac{1}{r^2}\int_0^r f(\rho)\rho d\rho, \tag{7a}$$

$$\sigma_{\theta\theta} = \tilde{A} + \tilde{B}\frac{1}{r^2} - 2\mu\frac{1+\nu}{1-\nu}\left[f(r) - \frac{1}{r^2}\int_0^r f(\rho)\rho d\rho \right], \tag{7b}$$

$$\sigma_{zz} = 2\nu\tilde{A} + 2\mu(1+\nu)e_{zz} - 2\mu\frac{1+\nu}{1-\nu}f(r). \tag{7c}$$

Here the following notations ar introduced:

$$\tilde{A} = 2\mu\frac{A + \nu e_{zz}}{1-2\nu}, \tag{8a}$$

$$\tilde{B} = 2\mu B. \tag{8b}$$

The unknown coefficients $\tilde{A}$, $\tilde{B}$ and axial strain e_{zz} can be obtained from the conditions

$$u(r \to 0) = \text{const}, \tag{9a}$$

$$\sigma_{rr}(r = b) = 0, \tag{9b}$$

$$2\pi \int_0^b \sigma_{zz} r dr = 0. \tag{9c}$$

The Eq. (9a) results in $B = 0$. Therefore, from Eq. (8b) we get:

$$\tilde{B} = 0. \tag{10a}$$

Now the coefficient $\tilde{A}$ can be derived from the traction boundary condition (9b) on the free cylindrical surface:

$$\tilde{A} = 2\mu\frac{1+\nu}{1-\nu}\frac{1}{b^2}\int_0^b f(\rho)\rho\, d\rho. \tag{10b}$$

The axial strain e_{zz} can be expressed from the equilibrium equation (9c) in integral form as:

$$e_{zz} = \frac{1-\nu}{1+\nu}\frac{\tilde{A}}{\mu}. \tag{10c}$$

For axial stress σ_{zz} one can obtain from the Eqs. (7) with respect to Eq. (10c):

$$\sigma_{zz} = \sigma_{rr} + \sigma_{\theta\theta} = 2\tilde{A} - 2\mu\frac{1+\nu}{1-\nu}f(r). \tag{11}$$

In order to investigate the influence of core and shell interface distinctness on the residual stress state of core-shell NWs (see Eqs. (7)) the different approximations are considered below.

The Heaviside theta function representation of misfit profile f is the simplest and the most effective approximation to describe the sharp interfaces, if the mutual penetration of core and shell atoms is negligibly small:

$$f_1(t) = f_0\Theta(t_0 - t), \tag{12}$$

where $t = r/b$ is a normalized radius, $t_0 = a/b$ is interface to NW ratio, f_0 is misfit parameter and Θ is a Heaviside theta function.

In contrast to sharp interfaces, the diffuse interfaces are distinguished by a significant mutual penetration of core and shell atoms. The following approximations of eigenstrain profiles in core-shell NWs can be employed to investigate the residual stress state of diffuse interfaces (see Fig. 2):

Piecewise-linear function

$$f_2(t) = f_0\begin{cases} 1, & 0 < t \le t_0 - \delta/2, \\ (t_0 - t)/\delta + 1/2, & t_0 - \delta/2 < t < t_0 + \delta/2, \\ 0, & t \ge t_0 + \delta/2, \end{cases} \tag{13}$$

Error function

$$f_3(t) = \frac{1}{2}f_0\left(1 + \operatorname{erf}\left[\frac{t_0 - t}{\alpha}\right]\right), \tag{14}$$

Arctangent function

$$f_4(t) = f_0\left(\frac{1}{2} + \frac{1}{\pi}\arctan\left[\frac{t_0 - t}{\beta}\right]\right), \tag{15}$$

where δ is the interface width normalized to the radius of NW, α and β are parameters defining the distinctness of interface.
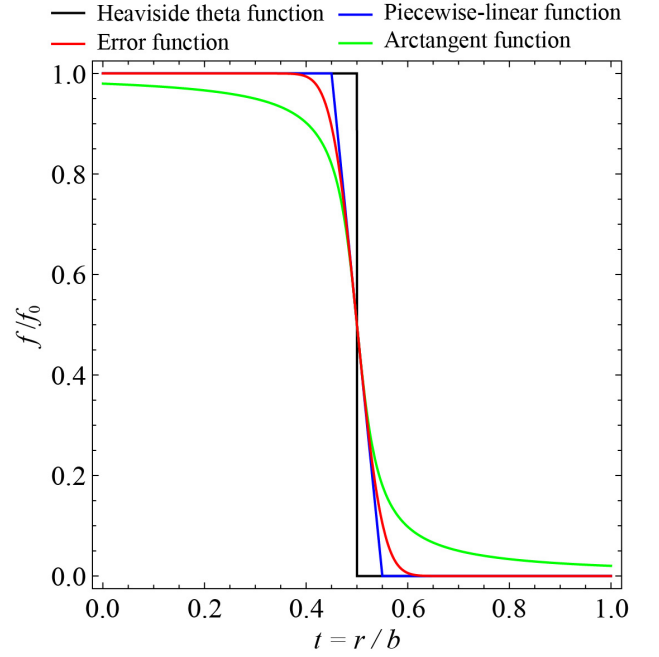

Fig. 2. Dependencies of the normalized eigenstrain deformation function f/f_0 on normalized radial coordinate $t = r/b$ in core-shell NWs. Here black, blue, red and green curves correspond to Heaviside theta, piecewise-linear ($\delta = 0.1$), error ($\alpha = 0.1/\pi^{1/2}$), and arctangent ($\beta = 0.1/\pi$) eigenstrain deformation functions respectively.

Introducing the expressions for approximations under consideration (12–15) in Eqs. (7) with regard to Eqs. (10) and Eq. (11) one can obtain the analytical solution of the elastic problem of core-shell NW subjected to inhomogeneous dilatational eigenstrain $f(r)$. The analytical expressions of the elastic stress are given in Appendix A.

3. RESULTS AND DISCUSSION

In further analysis of elastic stresses (A.2–A.4) in core-shell NWs, the approximations describing the diffuse (piecewise, error, arctangent functions) and sharp (Heaviside theta function) interfaces are presumed to have a common tangent line at the core-shell boundary ($t = t_0$) as it is shown in Fig. 2.

The distributions of the radial stress σ_{rr} in core-shell NW for different eigenstrain approximations are depicted in Fig. 3. The fulfillment of boundary condition (9b) at the outer cylindrical surface ($t = 1$) for all approximations is demonstrated. As it is seen from Fig. 3 the curves of diffuse IPhBs significantly differ from the curve of sharp IPhBs in the vicinity of interface ($t = t_0$). Besides, the arctangent approximation for given parameters takes less absolute value of radial stress in core region then it is predicted by other approximations. This discrepancy can be explained by the fact that the value of ratio f/f_0 for arctangent function is not close enough to other approximations at $t = 0$ and $t = 1$
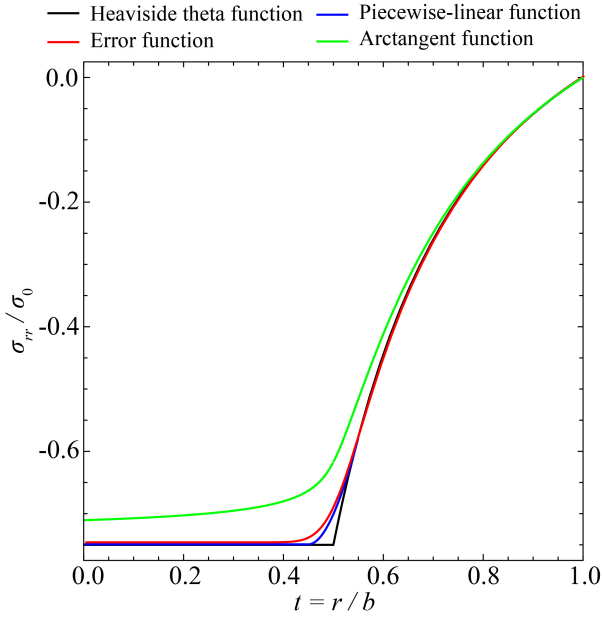
Fig. 3. Dependencies of the normalized radial stress components σ_{rr} / σ_0 on normalized radial coordinate $t = r / b$ in core-shell NWs. Here black, blue, red and green curves correspond to Heaviside theta, piecewise-linear ($\delta = 0.1$), error ($\alpha = 0.1 / \pi^{1/2}$), and arctangent ($\beta = 0.1 / \pi$) eigenstrain deformation functions respectively.

Fig. 4. Dependencies of the normalized hoop stress components $\sigma_{\theta\theta} / \sigma_0$ on normalized radial coordinate $t = r / b$ in core-shell NWs. Here black, blue, red and green curves correspond to Heaviside theta, piecewise-linear ($\delta = 0.1$), error ($\alpha = 0.1 / \pi^{1/2}$), and arctangent ($\beta = 0.1 / \pi$) eigenstrain deformation functions respectively.
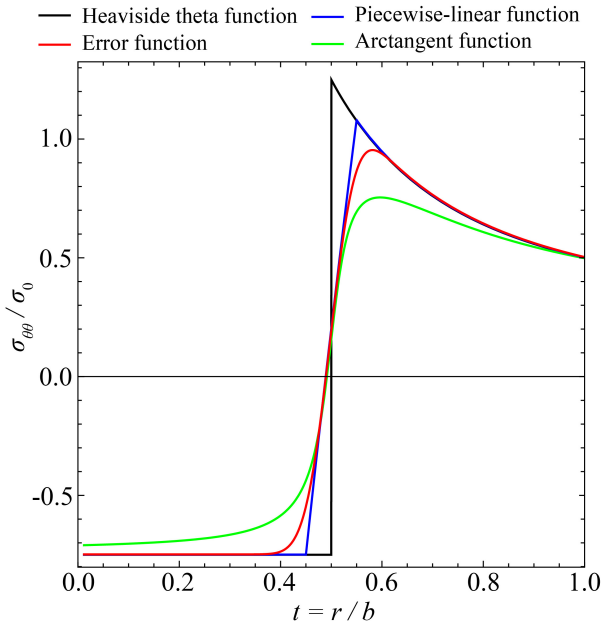
for prescribed parameter $\beta = \delta / \pi$ (see Fig. 2) and can be eliminated if parameter β tends to 0.

The dependences of hoop stress $\sigma_{\theta\theta}$ on normalized radial coordinate t for different eigenstrain approximations in NW is illustrated in Fig. 4. What can be clearly seen in
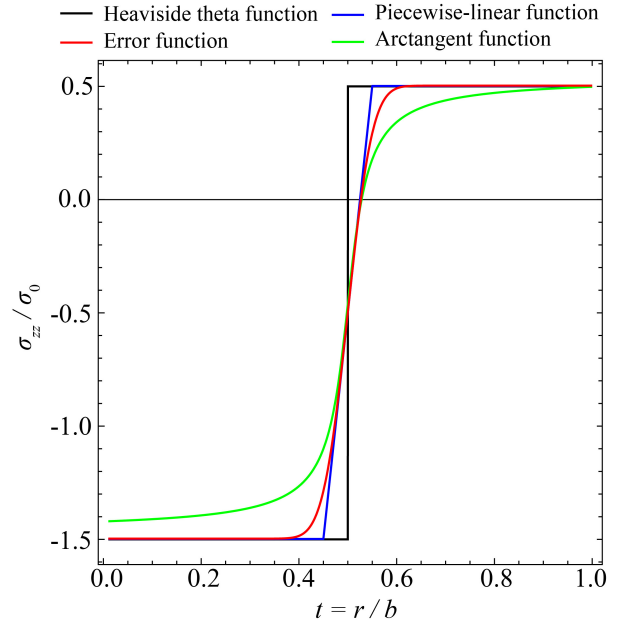

Fig. 5. Dependencies of the normalized axial stress components σ_{zz} / σ_0 on normalized radial coordinate $t = r / b$ in core-shell NWs. Here black, blue, red and green curves correspond to Heaviside theta, piecewise-linear ($\delta = 0.1$), error ($\alpha = 0.1 / \pi^{1/2}$), and arctangent ($\beta = 0.1 / \pi$) eigenstrain deformation functions respectively.

Fig. 4 is that for all approximations the local maximum is detected in the shell region. The peak stress decreases and shifts toward outer interface if the interface distinctness reduces.

The axial stress σ_{zz} in core-shell NW demonstrated in Fig. 5. It is proportional to the eigenstrain function $f(t)$ according to the Eq. (11). Therefore, the stress in NW with sharp interface is homogenous in core and shell, while the ones in NW with diffuse interface are inhomogeneous in core and shell.

As it seen from Figs. 3–5 the highest absolute values of stress components are observed in NW subjected to eigenstrain with Heaviside theta profile, whereas the lowest absolute values of stress components are detected in NW subjected to eigenstrain with arctangent function profile for given parameters of approximation.

4. CONCLUSIONS

In summary, the theoretical model describing the misfit stress of core-shell NWs containing the diffuse IPhBs with different range of distinctness has been proposed. We treated a core-shell NW as an elastic cylinder subjected to inhomogeneous eigenstrain determined by piecewise-linear, error and arctangent approximations. The nonzero components of stress tensor have been obtained analytically for aforementioned approximations. It has been shown that the stress concentration phenomenon is strongly depended on interface distinctness defined by eigenstrain profiles: the

less the interface distinctiveness, the less stress magnitude in NW. In case of eigenstrain functions with the same tangent at $t = t_0$, the lowest stress magnitudes correspond to the NW with arctangent approximation of eigenstrain deformation. Overall, it is worth noting that the piecewise linear eigenstrain approximation seems to be more effective to develop theoretical model of misfit stress relaxation in core-shell NWs with diffuse interface due to the facts that the misfit stress induced by the piecewise linear eigenstrain can be expressed in terms of power polynomials and parameter δ has a clear physical meaning of diffuse interface transient region.

ACKNOWLEDGEMENTS

APPENDIX A

Analytical expressions of the elastic stress tensor components in radial NWs subjected to inhomogeneous

dilatational eigenstrain demonstrated in Fig. 2 are introduced below.

The stress tensor components in core-shell NWs with the Heaviside theta eigenstrain profile attributed to the sharp interfaces are well-known (see, for example, Ref. [11]):

$$\sigma_{rr}^{(1)} = \sigma_0 \begin{cases} t_0^2 - 1, & 0 \le t \le t_0, \\ t_0^2 \left(1 - \dfrac{1}{t^2}\right), & t_0 < t \le 1, \end{cases} \tag{A.1a}$$

$$\sigma_{\theta\theta}^{(1)} = \sigma_0 \begin{cases} t_0^2 - 1, & 0 \le t \le t_0, \\ t_0^2 \left(1 + \dfrac{1}{t^2}\right), & t_0 < t \le 1, \end{cases} \tag{A.1b}$$

$$\sigma_{zz}^{(1)} = 2\sigma_0 \begin{cases} t_0^2 - 1, & 0 \le t \le t_0, \\ t_0^2, & t_0 < t \le 1, \end{cases} \tag{A.1c}$$

where $\sigma_0 = \mu f_0 (1+\nu)/(1-\nu)$.

The nonzero stress tensor components in core-shell NWs with piecewise-linear eigenstrain profile are obtained in this work as follows:

$$\sigma_{rr}^{(2)} = \sigma_0 \begin{cases} -1 + t_0^2 + \dfrac{\delta^2}{12}, & 0 \le t \le t_0 - \delta/2, \\ \dfrac{16t^3 + 2t^2(-12t_0 - 6\delta + 12t_0^2\delta + \delta^3) + (2t_0 - \delta)^3}{24t^2\delta}, & t_0 - \delta/2 < t \le t_0 + \delta/2, \\ \dfrac{(t^2-1)(12t_0^2 + \delta^2)}{12t^2}, & t_0 + \delta/2 < t \le 1, \end{cases} \tag{A.2a}$$

$$\sigma_{\theta\theta}^{(2)} = \sigma_0 \begin{cases} -1 + t_0^2 + \dfrac{\delta^2}{12}, & 0 \le t \le t_0 - \delta/2, \\ \dfrac{32t^3 + 2t^2(-12t_0 - 6\delta + 12t_0^2\delta + \delta^3) - (2t_0 - \delta)^3}{24t^2\delta}, & t_0 - \delta/2 < t \le t_0 + \delta/2, \\ \dfrac{(t^2+1)(12t_0^2 + \delta^2)}{12t^2}, & t_0 + \delta/2 < t \le 1, \end{cases} \tag{A.2b}$$

$$\sigma_{zz}^{(2)} = \sigma_0 \begin{cases} -2 + 2t_0^2 + \dfrac{\delta^2}{6}, & 0 \le t \le t_0 - \delta/2, \\ -1 + 2t_0^2 + \dfrac{2t}{\delta} - \dfrac{2t_0}{\delta} + \dfrac{\delta^2}{6}, & t_0 - \delta/2 < t \le t_0 + \delta/2, \\ 2t_0^2 + \dfrac{\delta^2}{6}, & t_0 + \delta/2 < t \le 1. \end{cases} \tag{A.2c}$$

The nonzero stress tensor components in core-shell NWs with error function eigenstrain profile are obtained in this work as follows:

$$\sigma_{rr}^{(3)} = \sigma_0 \left(\dfrac{2(t^2 - t_0^2) - \alpha^2}{4t^2} \operatorname{erf}\dfrac{t - t_0}{\alpha} - \dfrac{2(1 - t_0^2) - \alpha^2}{4} \operatorname{erf}\dfrac{1 - t_0}{\alpha} \right.$$

$$+ \dfrac{(2t_0^2 + \alpha^2)(t^2 - 1)}{4t^2} \operatorname{erf}\dfrac{t_0}{\alpha} + \dfrac{\alpha(t + t_0)}{2\sqrt{\pi}t^2} \exp\left[-\dfrac{(t - t_0)^2}{\alpha^2} \right]$$

$$\left. - \dfrac{\alpha(1 + t_0)}{2\sqrt{\pi}} \exp\left[-\dfrac{(1 - t_0)^2}{\alpha^2} \right] + \dfrac{\alpha t_0(t^2 - 1)}{2\sqrt{\pi}t^2} \exp\left[-\dfrac{t_0^2}{\alpha^2} \right] \right), \tag{A.3a}$$

$$\sigma_{\theta\theta}^{(3)} = \frac{\sigma_0}{4}\left\{\frac{2(t^2+t_0^2)+\alpha^2}{t^2}\operatorname{erf}\frac{t-t_0}{\alpha}+(2t_0^2+\alpha^2-2)\operatorname{erf}\frac{1-t_0}{\alpha}\right.$$

$$+\frac{(t^2+1)(2t_0^2+\alpha^2)}{t^2}\operatorname{erf}\frac{t_0}{\alpha}+\frac{2}{\sqrt{\pi}t^2}\left(-(t+t_0)\alpha\exp\left[-\frac{(t-t_0)^2}{\alpha^2}\right]\right.$$

$$\left.\left.-t^2\alpha(1+t_0)\exp\left[-\frac{(1-t_0)^2}{\alpha^2}\right]+t_0\alpha(t^2+1)\exp\left[-\frac{t_0^2}{\alpha^2}\right]\right)\right\},$$

$$\text{(A.3b)}$$

$$\sigma_{zz}^{(3)} = \frac{\sigma_0}{2}\left(2\operatorname{erf}\frac{t-t_0}{\alpha}+(2t_0^2+\alpha^2-2)\operatorname{erf}\frac{1-t_0}{\alpha}+(2t_0^2+\alpha^2)\operatorname{erf}\frac{t_0}{\alpha}\right.$$

$$\left.+\frac{2t_0\alpha}{\sqrt{\pi}}\exp\left[-\frac{t_0^2}{\alpha^2}\right]-\frac{2\alpha(1+t_0)}{\sqrt{\pi}}\exp\left[-\frac{(1-t_0)^2}{\alpha^2}\right]\right). \quad \text{(A.3c)}$$

The nonzero stress tensor components in core-shell NWs with arctangent function eigenstrain profile are obtained in this work as follows:

$$\sigma_{rr}^{(4)} = \frac{\sigma_0}{\pi}\left\{\frac{\beta(t-1)}{t}+t_0\beta\left(\frac{1-t^2}{t^2}\ln\left[t_0^2+\beta^2\right]-\frac{1}{t^2}\ln\left[(t-t_0)^2+\beta^2\right]\right.\right.$$

$$\left.+\ln\left[(1-t_0)^2+\beta^2\right]\right)+\frac{t^2-t_0^2+\beta^2}{t^2}\arctan\frac{t-t_0}{\beta}$$

$$\left.+(t_0^2-\beta^2-1)\arctan\frac{1-t_0}{\beta}+\frac{(\beta^2-t_0^2)(1-t^2)}{t^2}\arctan\frac{t_0}{\beta}\right\},$$

$$\text{(A.4a)}$$

$$\sigma_{\theta\theta}^{(4)} = \frac{\sigma_0}{\pi}\left\{\frac{\beta(t+1)}{t}+t_0\beta\left(-\frac{t^2+1}{t^2}\ln\left[t_0^2+\beta^2\right]+\frac{1}{t^2}\ln\left[(t-t_0)^2+\beta^2\right]\right.\right.$$

$$\left.+\ln\left[(1-t_0)^2+\beta^2\right]\right)+\frac{t^2+t_0^2-\beta^2}{t^2}\arctan\frac{t-t_0}{\beta}$$

$$\left.+(t_0^2-\beta^2-1)\arctan\frac{1-t_0}{\beta}-\frac{(\beta^2-t_0^2)(t^2+1)}{t^2}\arctan\frac{t_0}{\beta}\right\},$$

$$\text{(A.4b)}$$

$$\sigma_{zz}^{(4)} = \frac{2\sigma_0}{\pi}\left\{\beta+t_0\beta\left(\ln\left[(1-t_0)^2+\beta^2\right]-\ln\left[t_0^2+\beta^2\right]\right)\right.$$

$$\left.+\arctan\frac{t-t_0}{\beta}+(t_0^2-\beta^2-1)\arctan\frac{1-t_0}{\beta}+(t_0^2-\beta^2)\arctan\frac{t_0}{\beta}\right\}.$$

$$\text{(A.4c)}$$

REFERENCES

[1] M.S. Gudiksen, L.J. Lauhon, J. Wang, D.C. Smith, C.M. Lieber, *Growth of nanowire superlattice structures for nanoscale photonics and electronics*, Nature, 2002, vol. 415, no. 6872, pp. 617–620.

[2] G. Priante, F. Glas, G. Patriarche, K. Pantzas, F. Oehler, J.-C. Harmand, *Sharpening the interfaces of axial heterostructures in self-catalyzed AlGaAs nanowires: experiment and theory*, Nano Lett., 2016, vol. 16, no. 3, pp. 1917–1924.

[3] V. Zannier, F. Rossi, V.G. Dubrovskii, D. Ercolani, S. Battiato, L. Sorba, *Nanoparticle stability in axial InAs–InP nanowire heterostructures with atomically sharp interfaces*, Nano Lett., 2018, vol. 18, no. 1, pp. 167–174.

[4] D.V. Beznasyuk, P. Stepanov, J.L. Rouvière, F. Glas, M. Verheijen, J. Claudon, M. Hocevar, *Full characterization and modeling of graded interfaces in a high lattice-mismatch axial nanowire heterostructure*, Phys. Rev. Mater., 2020, vol. 4, no. 7, art. no. 074607.

[5] V.G. Dubrovskii, A.A. Koryakin, N.V. Sibirev, *Understanding the composition of ternary III-V nanowires and axial nanowire heterostructures in nucleation-limited regime*, Mater. Des., 2017, vol. 132, pp. 400–408.

[6] A.E. Romanov, A.L. Kolesnikova, M.Yu. Gutkin, V.G. Dubrovskii, *Elasticity of axial nanowire heterostructures with sharp and diffuse interfaces*, Scr. Mater., 2020, vol. 176, pp. 42–46.

[7] A.E. Romanov, A.L. Kolesnikova, M.Yu. Gutkin, *Elasticity of a cylinder with axially varying dilatational eigenstrain*, Int. J. Solids Struct., 2021, vol. 213, pp. 121–134.

[8] A.L. Kolesnikova, M.Yu. Gutkin, A.E. Romanov, V.E. Bougrov, *Strain energy in hybrid nanowire structures with axially varying eigenstrain*, Int. J. Solids Struct., 2022, vol. 254–255, art. no. 111819.

[9] V.G. Dubrovskii, *Understanding the vapor-liquid-solid growth and composition of ternary III-V nanowires and nanowire heterostructures*, J. Phys. D: Appl. Phys., 2017, vol. 50, no. 45, art. no. 453001.

[10] A.M. Smirnov, S.A. Krasnitckii, S.S. Rochas, M.Yu. Gutkin, *Critical conditions of dislocation generation in core-shell nanowires: A review*, Rev. Adv. Mater. Technol., 2020, vol. 2, no. 3, pp. 19–43.

[11] S.A. Krasnitckii, A.M. Smirnov, M.Yu. Gutkin, *Axial misfit stress relaxation in core–shell nanowires with polyhedral cores through the nucleation of misfit prismatic dislocation loops*, J. Mater. Sci., 2020, vol. 55, no. 22, pp. 9198–9210.

[12] A.M. Smirnov, S.A. Krasnitckii, M.Yu. Gutkin, *Generation of misfit dislocations in a core-shell nanowire near the edge of prismatic core*, Acta Mater., 2020, vol. 186, pp. 494–510.

[13] S.A. Krasnitckii, A.M. Smirnov, K.D. Mynbaev, L.V. Zhigilei, M.Yu. Gutkin, *Axial misfit stress relaxation in core-shell nanowires with hexagonal core via nucleation of rectangular prismatic dislocation loops*, Mater. Phys. Mech., 2019, vol. 42, no. 6, pp. 776–783.

[14] S.A. Krasnitckii, D.R. Kolomoetc, A.M. Smirnov, M.Yu. Gutkin, *Misfit stress relaxation in composite core-shell nanowires with parallelepiped cores using rectangular prismatic dislocation loops*, J. Phys. Conf. Ser., 2018, vol. 993, no. 1, art. no. 012021.

[15] S.A. Krasnitckii, D.R. Kolomoetc, A.M. Smirnov, M.Yu. Gutkin, *Misfit stresses in a composite core-shell nanowire with an eccentric parallelepipedal core subjected to one-dimensional cross dilatation eigenstrain*, J. Phys. Conf. Ser., 2017, vol. 816, no. 1, art. no. 012043.

[16] M.Yu. Gutkin, A.M. Smirnov, *Initial stages of misfit stress relaxation through the formation of prismatic dislocation loops in GaN–Ga2O3 composite nanostructures*, Phys. Solid State, 2016, vol. 58, no. 8, pp. 1611–1621.

[17] M.Yu. Gutkin, S.A. Krasnitckii, A.M. Smirnov, A.L. Kolesnikova, A.E. Romanov, *Dislocation loops in solid*

and hollow semiconductor and metal nanoheterostructures, Phys. Solid State, 2015, vol. 57, no. 6, pp. 1177–1182.

[18] M.Yu. Gutkin, A.M. Smirnov, *Initial stages of misfit stress relaxation by rectangular prismatic dislocation loops in composite nanostructures*, J. Phys. Conf. Ser., 2014, vol. 541, no. 1, art. no. 012007.

[19] G. Perillat-Merceroz, R. Thierry, P.-H. Jouneau, P. Ferret, G. Feuillet, *Strain relaxation by dislocation glide in ZnO/ZnMgO core-shell nanowires*, Appl. Phys. Lett., 2012, vol. 100, no. 17, art. no. 173102.

[20] M.Yu. Gutkin, K.V. Kuzmin, A.G. Sheinerman, *Misfit stresses and relaxation mechanisms in a nanowire containing a coaxial cylindrical inclusion of finite height*, Phys. Status Solidi, 2011, vol. 248, no. 7, pp. 1651–1657.

[21] J. Colin, *Prismatic dislocation loops in strained core-shell nanowire heterostructures*, Phys. Rev. B, 2010, vol. 82, no. 5, art. no. 054118.

[22] K.E. Aifantis, A.L. Kolesnikova, A.E. Romanov, *Nucleation of misfit dislocations and plastic deformation in core/shell nanowires*, Philos. Mag., 2007, vol. 87, no. 30, pp. 4731–4757.

[23] S. Raychaudhuri, E.T. Yu, *Critical dimensions in coherently strained coaxial nanowire heterostructures*, J. Appl. Phys., 2006, vol. 99, no. 11, art. no. 114308.

[24] I.A. Ovid'ko, A.G. Sheinerman, *Misfit dislocation loops in composite nanowires*, Philos. Mag., 2004, vol. 84, no. 20, pp. 2103–2118.

[25] A.G. Sheinerman, M.Yu. Gutkin, *Misfit disclinations and dislocation walls in a two-phase cylindrical composite*, Phys. Status Solidi, 2001, vol. 184, no. 2, pp. 485–505.

[26] M.Yu. Gutkin, I.A. Ovid'ko, A.G. Sheinerman, *Misfit dislocations in wire composite solids*, J. Phys. Condens. Matter., 2000, vol. 12, no. 25, pp. 5391–5401.

Напряжения несоответствия в радиальных нанопроволоках типа «ядро-оболочка» с диффузными границами раздела

А.С. Храмов[1], С.А. Красницкий[1–4], А.М. Смирнов[1]

[1] Институт перспективных систем передачи данных Университета ИТМО, Кронверкский пр., д. 49, лит А, Санкт-Петербург, 197101, Россия

[2] Лаборатория механики наноматериалов и теории дефектов ИПМаш РАН, Большой пр., д. 61, Санкт-Петербург, 199178, Россия

[3] Лаборатория механики новых материалов, СПбПУ Петра Великого, Политехническая ул., д. 29, Санкт-Петербург, 195251, Россия

[4] Кафедра вычислительных методов механики деформируемого тела СПбГУ, Университетская наб., д. 7-9, Санкт-Петербург, 199034, Россия

Аннотация. Предложены упругие модели радиальных нанопроволок типа «ядро-оболочка» с диффузными межфазными границами различной степени размытости. Распределение напряжений несоответствия в подобных нанопроволоках описано на основе концепции собственной деформации, которая определялась с помощью параметра несоответствия и аппроксимировалась кусочно-линейной функцией, функцией ошибки и арктангенсом. В рамках указанных аппроксимаций проведен подробный анализ поля упругих напряжений в нанопроволоках типа «ядро-оболочка», получены соответствующие зависимости и аналитические выражения.

Ключевые слова: нанопроволока типа «ядро-оболочка»; диффузные границы; напряжения несоответствия